Mean-Square Optical Anisotropy of Oligo- and Poly(methyl methacrylate)s in Dilute Solutions

Yoshio Takaeda, Takenao Yoshizaki, and Hiromi Yamakawa*

Department of Polymer Chemistry, Kyoto University, Kyoto 606-01, Japan

Received December 9, 1992; Revised Manuscript Received April 16, 1993

ABSTRACT: The mean-square optical anisotropy $\langle\Gamma^2\rangle$ was determined for 10 samples of atactic oligo- and poly(methyl methacrylate)s (a-PMMA), each with the fraction of racemic diads $f_r = 0.79$, in the range of weight-average molecular weight M_w from 3.02×10^2 to 2.95×10^3 in acetonitrile at 44.0 °C (Θ) and also for methyl isobutyrate (MIB) (the monomer of PMMA) in acetonitrile at 44.0 °C and in carbon tetrachloride at 25.0 °C, from anisotropic light scattering measurements with a photometer equipped with a Fabry–Perot interferometer. The determination was also made for three samples of atactic oligo- and polystyrenes (a-PS) used in the previous study of $\langle\Gamma^2\rangle$ along with cumene in carbon tetrachloride at 25.0 °C in order to compare the present procedure for determining $\langle\Gamma^2\rangle$ with the previous one. A comparison is made of the present data with the helical wormlike (HW) chain theory with the values of the model parameters determined previously from the mean-square radius of gyration $\langle S^2\rangle$ and with the local polarizability tensor α_0 properly assigned on the basis of the group polarizability tensor for the ester group of the a-PMMA chain evaluated from the polarizability of methyl acetate or MIB. The HW theoretical value of the ratio $(\langle\Gamma^2\rangle/x_w)_\infty$ in the limit of weight-average degree of polymerization $x_w \to \infty$ does not completely agree with the experimental one if such α_0 is used. This is probably due to the fact that the group polarizability of the ester group may be somewhat altered in the a-PMMA chain. The dependence on x_w of the observed ratio $(\langle\Gamma^2\rangle/x_w)/(\langle\Gamma^2\rangle/x_w)_\infty$ may well be explained by the HW theory, thus leading to the conclusion that the HW model may give a consistent explanation of the behavior of $\langle\Gamma^2\rangle$ and $\langle S^2\rangle$ of a-PMMA. A comparison is also made of the present results for a-PMMA with the previous ones for a-PS; as x_w is decreased to 3, the above ratio decreases much more steeply for the former.

Introduction

In this series of experimental work on dilute solutions of oligomers and polymers in the unperturbed (Θ) state, we have investigated static and/or transport properties of atactic polystyrene (a-PS) (with the fraction of racemic diads $f_r = 0.59$),[1] atactic poly(methyl methacrylate) (a-PMMA) (with $f_r = 0.79$),[2,3] polyisobutylene,[4] and poly(dimethylsiloxane).[5] It has been shown that the results obtained may well be explained by the corresponding theories on the basis of the helical wormlike (HW) chain,[6,7] with a rather accurate determination of the model parameters for these polymer chains. With their values determined, the local chain conformations have been discussed in some detail in their relations to solution properties. In particular, for a-PS, we have started with an analysis of the data obtained for the mean-square optical anisotropy $\langle\Gamma^2\rangle$ from anisotropic light scattering (LS) measurements,[1] and it has proved to be one of the useful properties that provide information about local chain conformations. Thus, in this paper, we make a study of $\langle\Gamma^2\rangle$ also for a-PMMA, for which we have already analyzed the data[2,3] obtained for the mean-square radius of gyration $\langle S^2\rangle$ and the intrinsic viscosity $[\eta]$.

In the previous determination of $\langle\Gamma^2\rangle$ for a-PS,[1] the experimental procedure proposed by Carlson and Flory[8] to eliminate the collision-induced polarizability contribution to anisotropic LS has been applied with the use of a Fica 50 photometer having a mercury lamp as a light source, with a modification suitable for this purpose. However, the a-PMMA chain has an optical anisotropy much smaller than that of the a-PS chain, so that it is difficult to determine accurately $\langle\Gamma^2\rangle$ of the former by the use of that photometer, whose light source is not as strong as a laser used by Carlson and Flory. Moreover, the optical anisotropy of acetonitrile to be used as a Θ solvent for a-PMMA is rather large compared to that of cyclohexane, the Θ solvent used in the previous study of a-PS,[1] and is even larger than that of a-PMMA. Thus, for an accurate determination of the excess depolarized scattering intensity for a-PMMA in acetonitrile, it is desirable to measure, instead of the integrated total intensity, the spectra of the light scattered from the solution and solvent, using a spectrometer appropriate for a photometer adopted.

In this work, we carry out anisotropic LS measurements by the use of a photometer originally designed for dynamic LS measurements by the homodyne method. Thus we have decided to use as a spectrometer a Fabry–Perot (FP) interferometer of the piezoelectrically scanning type, which may be considered most suitable for the present purpose because of its handiness and compactness. Then the photometer has been equipped with a newly assembled detector alignment in order to incorporate an FP interferometer in it. We note that the interferometer of this type has been widely used in dynamic LS measurements by the filter method[9] and in studies of Rayleigh–Brillouin scattering by polymer melts[10] and anisotropic LS by polymer solutions.[11]

The spectrum of the excess depolarized component of the light scattered from the solute a-PMMA molecules may be determined apparently from the FP spectra. However, we must be careful in doing this in the case of an optically anisotropic solvent, i.e., acetonitrile, since the solvent molecules of this kind have in general orientational correlations with each other[12] and an addition of solute molecules to them may have an effect on those correlations enough to change the spectrum of the light scattered from them. Thus, in order to examine possible effects of the optical anisotropy of the solvent on the evaluation of $\langle\Gamma^2\rangle$, it is desirable to carry out measurements also for solutions in an optically isotropic solvent, e.g., carbon tetrachloride, and to compare the results with those for acetonitrile solutions. For this purpose, we have carried out some preliminary measurements for the carbon tetrachloride solutions. Unfortunately, however, the exposure of these solutions of a-PMMA samples to a strong laser beam has

0024-9297/93/2226-3742$04.00/0

Table I. Values of M_w, x_w, and M_w/M_n for Atactic Oligo- and Polystyrenes

sample	M_w	x_w	M_w/M_n
OS3[a]	3.70×10^2	3	1.00
OS4	4.74×10^2	4	1.00
A5000-3[b]	5.38×10^3	51.2	1.03

[a] M_w's of OS3 and OS4 had been determined from GPC.[1] [b] M_w of A5000-3 had been determined from LS in methyl ethyl ketone at 25.0 °C.[1]

Table II. Values of M_w, x_w, and M_w/M_n for Atactic Oligo- and Poly(methyl methacrylate)s

sample	M_w	x_w	M_w/M_n
OM3[a]	3.02×10^2	3	1.00
OM4	4.02×10^2	4	1.00
OM5	5.02×10^2	5	1.00
OM6	6.02×10^2	6.00	1.00
OM7	7.09×10^2	7.07	1.00
OM8	7.98×10^2	7.96	1.00
OM11[b]	1.10×10^3	11.0	1.04
OM18	1.80×10^3	18.0	1.07
OM22	2.23×10^3	22.3	1.06
OM30	2.95×10^3	29.5	1.06

[a] M_w's of OM3 through OM8 had been determined from GPC.[2,3] [b] M_w's of OM11 through OM30 had been determined from LS in acetone at 25.0 °C.[2]

proved to denature the precious samples and prevent their reuse. Therefore, the examination has been restricted to the monomer of PMMA, i.e., methyl isobutyrate.

We have carried out measurements also for some of the a-PS samples previously used in order to compare the present procedure for determining $\langle\Gamma^2\rangle$ with the previous one. With the new photometer, it may be determined rather accurately even for a-PMMA, but its accuracy is still somewhat worse than that for the case of a-PS. Further, in anticipation of the results, we note that it is difficult to determine unambiguously all the HW model parameters for a-PMMA from an analysis of the molecular weight dependence of $\langle\Gamma^2\rangle$ alone. In this paper, therefore, we examine whether the dependence of $\langle\Gamma^2\rangle/x$ on the degree of polymerization x may well be explained by the HW theory[13] with the values of the model parameters determined previously from $\langle S^2\rangle$.[2]

Experimental Section

Materials. All the a-PS and a-PMMA samples used in this work are the same as those used in the previous studies,[1-3] i.e., the fractions separated by gel permeation chromatography (GPC) and/or fractional precipitation from the standard a-PS samples A-500 and A-5000 supplied by Tosoh Co., Ltd., and from the original a-PMMA samples prepared by group-transfer polymerization, respectively. The values of the weight-average molecular weight M_w, the weight-average degree of polymerization x_w, and the ratio of M_w to the number-average molecular weight M_n are given in Table I for the a-PS samples and in Table II for the a-PMMA samples.

Methyl isobutyrate (MIB) (Tokyo Kasei Kogyo Co.; 99.0% purity), the monomer of PMMA, was purified by distillation after dehydration by passing through a silica gel column. Cumene, which corresponds to the monomer of PS, and the solvents carbon tetrachloride (CCl_4) and acetonitrile (CH_3CN) were purified according to standard procedures.

Anisotropic Light Scattering. (i) Apparatus and Measurements. The photometer used for all anisotropic LS measurements is a Brookhaven Instruments Model BI-200SM goniometer with a minor modification of its light source part and with a detector alignment newly assembled to incorporate an FP interferometer in it.

In Figure 1 is depicted a block diagram of the photometer with the FP scan generator and photon counter units. The formation

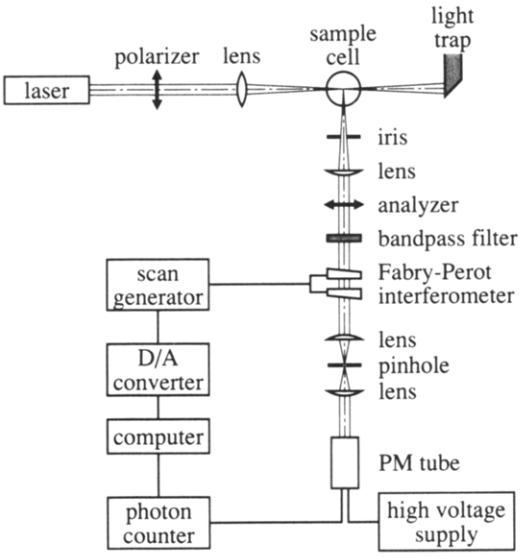

Figure 1. Block diagram of the anisotropic light scattering apparatus.

of the detector alignment adopted here is similar to that reported by Patterson,[10] it being fixed at a right angle with respect to the incident light. The vertically polarized incident light beam of wavelength 488 nm from a Spectra-Physics Model 2020 argon ion laser equipped with a Model 583 temperature-stabilized etalon for single-frequency-mode operation is first made highly vertically (v) polarized by passing through a polarizer, a Glan-Thompson (GT) prism with an extinction ratio smaller than 10^{-5}, and then focused at the center of a cylindrical sample cell of outer diameter 25 mm by a biconvex lens of focal length 113 mm. (Note that the polarizer has been newly introduced.) After passing through an iris, the light scattered from the center of the cell is rendered a parallel light beam of diameter ca. 5 mm by a plano-convex lens of focal length 200 mm and then its vertical component is eliminated by an analyzer, the same GT prism as used for the polarizer. A narrow band-pass filter with full width at half-maximum of ca. 110 cm^{-1} is incorporated into the alignment in order to remove possible effects of the Raman scattering and background fluorescence. The spectrum of the horizontal (H) component of the scattered light, i.e., the depolarized (Hv) component, is then analyzed with a Burleigh Instruments Model RC-110 FP interferometer (piezoelectrically scanned) equipped with a Model RC-670 pair of plane mirrors with a flatness of $\lambda/200$ and a reflectivity of 97.5%. The light beam, which has passed through the FP interferometer, then passes through a spatial filter composed of a pair of plano-convex lenses of focal length 40 mm and a pinhole of diameter 100 μm placed in the middle of them and is finally imaged on an EMI 9893B/350 photomultiplier (PM) tube.

After passing through an amplifier/discriminator, the signal from the PM tube enters a photon counter, for which a Brookhaven Instruments Model BI2030AT autocorrelator is used. The FP interferometer is scanned by the use of a Burleigh Instruments Model RC-44 scan generator driven with an external direct-current signal which is generated by a computer with a 12-bit digital-to-analog (D/A) converter, so that it may be scanned with 4096 steps at maximum. The total number of photons accumulated at a (identical) time interval δ at each step is successively stored in the computer. In practice, a frequency range of twice the free spectral range (FSR) was scanned with 1024 steps and $\delta = 0.1$ s, so that it took ca. 150 s for each scan.

The apparatus is installed in a temperature-controlled room (at 25 ± 1 °C) so that the fluctuation in the cavity length of the FP interferometer due to thermal expansion of its frame and that in effective optical path length in the cavity due to change of the air density may be neglected.

The most concentrated solution of each sample was prepared gravimetrically and made homogeneous by continuous stirring for ca. 1 day at room temperature for a-PS and at ca. 50 °C for a-PMMA. These solutions and solvents were optically purified by filtration through a Teflon membrane of pore size 0.1 μm. The

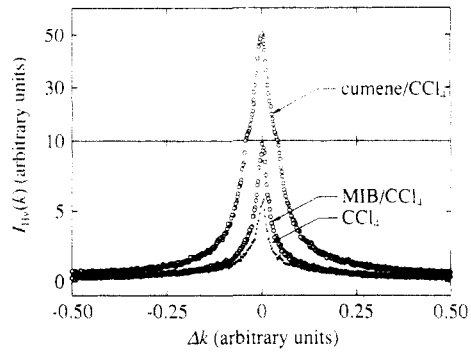

Figure 2. Fabry–Perot spectra of depolarized light scattered from CCl_4 and its solutions of cumene and MIB at 25.0 °C, their mass concentrations c being 0.1837 and 0.1787 g/cm³, respectively.

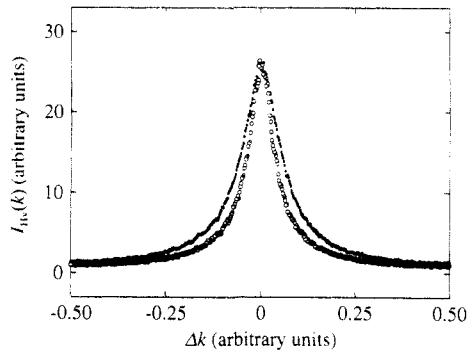

Figure 3. Fabry–Perot spectra of depolarized light scattered from CH_3CN (●) and its solution of MIB at c = 0.4013 g/cm³ (○) at 44.0 °C.

solutions of lower concentrations were obtained by successive dilution. As for the solutions of cumene and MIB, the solute was filtered and added to the purified solvent in a sample cell. The weight concentrations of the test solutions were converted to the solute mass concentrations c (in g/cm³) by the use of the densities of the solutions.

Before and after each measurement on the solution or solvent, the spectrum of the Hv component scattered from pure benzene sealed in a Pyrex nuclear magnetic resonance tube of outer diameter 10 mm, which we used as a working standard (WS), was measured without the narrow band-pass filter in order to monitor any possible changes in the photometer system. Before every set of three measurements on pure benzene, on solution or solvent, and again on benzene, the FP interferometer was tuned to obtain the highest finesse. The value of the finesse was 60–70 just after the tuning and usually decreased to 40–50 after the set of measurements, which took ca. 1 h. The FSR was adjusted to be 5–50 cm⁻¹.

(ii) Data Acquisition and Analysis. Figure 2 shows FP spectra of the depolarized component $I_{Hv}(\Delta k)$ of the scattered light intensity as a function of the wave number difference Δk between the incident and scattered light in the range of one FSR for CCl_4 and its solutions of cumene at c = 0.1837 g/cm³ and of MIB at c = 0.1787 g/cm³ at 25.0 °C, and Figure 3 shows those for CH_3CN and its solution of MIB at c = 0.4013 g/cm³ at 44.0 °C. All the values of I_{Hv} have been reduced by the total intensity of the Hv component for the WS determined from the measurements mentioned above. We note that the intensity was found to be almost independent of temperature in its range from 25.0 to 44.0 °C.

As mentioned in the Introduction, the depolarized scattering intensity from solutions in an optically anisotropic solvent may be affected by the change in the depolarized scattering from the solvent molecules themselves. Such a change may possibly occur even for the case of optically isotropic solvents, since the anisotropic fluctuation in the density of the pure solvent may give rise to anisotropic scattering and an addition of solute molecules may in general affect this fluctuation.[14,15] In practice, however, as far as optically isotropic solvents are concerned, this change must be small, so that the excess Hv component $\Delta I_{Hv}(\Delta k)$

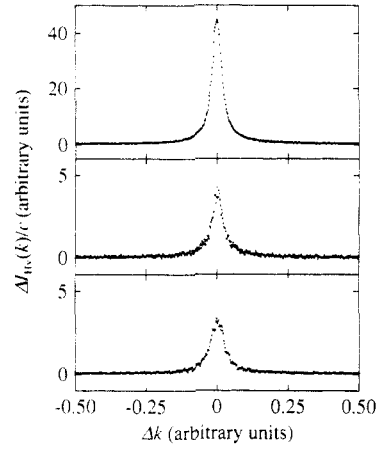

Figure 4. Fabry–Perot spectra of the excess depolarized scattered light. They are for cumene in CCl_4 at c = 0.1837 g/cm³ at 25.0 °C, for MIB in CCl_4 at c = 0.1787 g/cm³ at 25.0 °C, and for MIB in CH_3CN at c = 0.4013 g/cm³ at 44.0 °C, from top to bottom.

of the scattered light intensity may be calculated from[8]

$$\Delta I_{Hv}(\Delta k) = I_{Hv,soln}(\Delta k) - \phi I_{Hv,solv}(\Delta k) \quad (1)$$

with the values of $I_{Hv}(\Delta k)$ for the solution and solvent, where ϕ is the volume fraction of the solvent. Although eq 1 is not necessarily guaranteed in the case of optically anisotropic solvents, we may conclude that it is approximately valid if it gives the same value of $\langle\Gamma^2\rangle$ as that determined in an optically isotropic solvent. This working criterion is checked in the next section. Figure 4 shows spectra of $\Delta I_{Hv}(\Delta k)$ thus evaluated for the same solutions of cumene and MIB in CCl_4 as in Figure 2 and for the same solution of MIB in CH_3CN as in Figure 3, from top to bottom.

The total intensity $\Delta I_{Hv,mol}$ of the intrinsic molecular part of the excess Hv component may be obtained by integration of $[\Delta I_{Hv}(\Delta k) - I_{base}]$ over Δk in the range of one FSR as follows:

$$\Delta I_{Hv,mol} = \int_{FSR}[\Delta I_{Hv}(\Delta k) - I_{base}]\, d(\Delta k) \quad (2)$$

where I_{base} is the intensity of the flat base part of the FP spectrum, which includes all the contributions of $I_{Hv}(\Delta k)$ from the ranges of $|\Delta k|/FSR \geq 0.5$ and therefore arises from the scattering due to the collision-induced polarizability. In practice, the integration may be replaced by summation.

Now the intrinsic molecular excess Hv component $\Delta R_{Hv,mol}$ of the reduced intensity may be calculated from

$$\Delta R_{Hv,mol} = \frac{\tilde{n}^2\phi_A}{T_{max}}\Delta I_{Hv,mol} \quad (3)$$

with the value of $\Delta I_{Hv,mol}$ determined above, where $\tilde{n}$ is the refractive index of the solvent used, T_{max} is the maximum (or peak) transmittance of the narrow band-pass filter, and ϕ_A is the apparatus constant dependent on the photometer used. In eq 3, the $\tilde{n}^2$ correction of Hermans and Levinson[16] has been applied, and also a correction of the absorption by the narrow band-pass filter to $\Delta I_{Hv,mol}$ has been simply made by the factor $1/T_{max}$ since the width of the resultant spectrum of the excess scattering intensity (shown in Figure 4) is sufficiently narrow compared to the full width at half-maximum of the filter. The value of ϕ_A is usually determined so that the value of the Hv component $\tilde{n}_{(benzene)}^2\phi_A I_{Hv,(benzene)}$ of the reduced intensity of the light scattered from pure benzene measured at a scattering angle of 90° by the use of the photometer may coincide with the value of the Hv component $R_{Hv,(benzene)}$ of the reduced intensity determined absolutely, where $I_{Hv,(benzene)}$ is the (total) intensity of the Hv component measured under the same condition of the apparatus (including the sample cell) as in the case of the measurements on the test solutions but without the narrow band-pass filter.

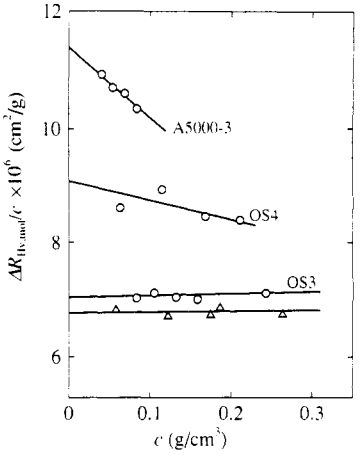

Figure 5. Plots of $\Delta R_{Hv,mol}/c$ against c for a-PS samples (○) in CCl_4 at 25.0 °C. The triangles represent the values for cumene.

Then ϕ_A may be obtained from

$$\phi_A = R_{Hv,(benzene)}/\tilde{n}_{(benzene)}{}^2 I_{Hv,(benzene)} \quad (4)$$

$R_{Hv,(benzene)}$ is a quantity depending only on the pressure, temperature, and wavelength of the incident light and must therefore be determined without a narrow band-pass filter, so that the intensity $I_{Hv,(benzene)}$ (relative to the WS) must also be determined without a narrow band-pass filter.

Although there have been reported some absolute values of the reduced intensities at λ_0 = 488 nm, from which we may evaluate $R_{Hv,(benzene)}$, we cannot decide which value is most reliable. Thus, in order to establish its value, we first determined the value of R_{Uv} for pure benzene at 25.0 °C and λ_0 = 488 nm in such a way that the value of M_w determined for a standard a-PS sample in benzene at 25.0 °C with the incident light of λ_0 = 488 nm may coincide with that determined with the incident light of λ_0 = 436 nm in the standard manner using a Fica 50 light scattering photometer in our laboratory.[2-4] This procedure is in principle the same as that adopted by Bender et al.,[17] who used a commercial standard a-PS sample with the nominal value 3.92×10^5 of M_w reported by Pressure Chemical Co.

For this purpose, we used an a-PS sample (F80a-2)[18] that was a fraction separated by fractional precipitation from the standard sample F-80 supplied by Tosoh Co., Ltd. The value of M_w of this sample had already been determined to be 7.32×10^5 with the ratio M_w/M_n = 1.03.[18] Static LS measurements of the Uv component (without use of a narrow band-pass filter) were carried out for the benzene solutions of the sample in the range of mass concentration c from 3.5×10^{-4} to 2.0×10^{-3} g/cm³ using the same photometer as that used for the present anisotropic LS measurements but with the standard detector alignment used for the previous dynamic LS measurements.[19,20] The scattered light intensities reduced by that for pure benzene at a scattering angle of 90° were analyzed by an application of the Berry square-root plot.[21] Thus the value of R_{Uv} was determined to be 39.8×10^{-6} cm⁻¹. This value is somewhat larger than the value 35.4×10^{-6} cm⁻¹ obtained by Bender et al.[17] The value of $R_{Hv,(benzene)}$ at 25.0 °C, scattering angle 90°, and λ_0 = 488 nm was then determined to be 8.16×10^{-6} cm⁻¹ from the value of R_{Uv} by use of the value 0.41 for the depolarization ratio ρ_u determined previously[2,4] for benzene at 25.0 °C and λ_0 = 436 nm. We note that ρ_u is almost independent of λ_0. Since $I_{Hv,(benzene)}$ is almost independent of temperature in its range from 25.0 to 44.0 °C as mentioned above, we used the value 8.16×10^{-6} cm⁻¹ of $R_{Hv,(benzene)}$ also at 44.0 °C.

The values of the refractive index we used for benzene at 25.0 °C, CCl_4 at 25.0 °C, and CH_3CN at 44.0 °C are 1.520, 1.465, and 1.337, respectively.

Results

Mean-Square Optical Anisotropy $\langle\Gamma^2\rangle$. (i) a-PS. For convenience, we begin by presenting results obtained for a-PS. Figure 5 shows plots of the ratio of the intrinsic molecular excess depolarized component $\Delta R_{Hv,mol}$ of the reduced intensity to the mass concentration c against c for the three a-PS samples indicated and cumene (triangles) in CCl_4 at 25.0 °C. The data points for each sample follow a straight line and can be rather easily extrapolated to infinite dilution to obtain $(\Delta R_{Hv,mol}/c)_{c=0}$. The error in the extrapolation for the sample OS4 is somewhat larger than those for the others. We note that the dependence on c of $\Delta R_{Hv,mol}/c$ for each sample is very similar to that reported previously.[1]

Table III. Values of $\langle\Gamma^2\rangle/x_w$ and $\langle\Gamma^2\rangle/\langle\Gamma^2\rangle_{(cumene)}$ for Atactic Oligo- and Polystyrenes in Carbon Tetrachloride at 25.0 °C

	$\langle\Gamma^2\rangle/x_w$, Å⁶		$\langle\Gamma^2\rangle/\langle\Gamma^2\rangle_{(cumene)}$	
sample	this work	previous work[a]	this work	previous work
cumene	$38_{.5}$	$19_{.8}$		
OS3	$41_{.1}$	$21_{.4}$	3.2_1	3.2_4
OS4	$50_{.8}$	$23_{.2}$	5.2_8	4.6_9
A5000-3	$56_{.6}$	$30_{.3}$	$75_{.4}$	$78_{.4}$

[a] See ref 1.

If the effect of the internal field is taken into account by the use of the Lorentz–Lorenz equation, the mean-square optical anisotropy $\langle\Gamma^2\rangle$ may be calculated from

$$\langle\Gamma^2\rangle = \frac{15\lambda_0^4}{16\pi^4}\frac{M}{N_A}\left(\frac{3}{\tilde{n}^2+2}\right)^2(\Delta R_{Hv,mol}/c)_{c=0} \quad (5)$$

with the observed value of $\Delta R_{Hv,mol}$ determined above, where λ_0 is the wavelength of the incident light in a vacuum and is equal to 488 nm, M is the solute molecular weight, N_A is Avogadro's number, and $\tilde{n}$ is the refractive index of the solvent. The adoption of the internal field correction of the second power type in eq 5 requires some comments. Brunham et al.[22] recommended the fourth-power-type correction along with the ellipsoidal Onsager–Scholte model on the basis of a detailed analysis of their data for isotropic and anisotropic components of the light scattered from several pure solvents. Strictly, however, the fourth-power-type "correction" factor appearing in the density scattering does not directly arise from a correction of the internal field but from the fact that the dependence of the refractive index of a pure solvent on the pressure may be described by the Lorentz–Lorenz equation.[23] Then, their results do not necessarily support the adoption of the fourth-power-type correction for the case of the composition scattering. Further, the value of the depolarization ratio ρ_u evaluated from their observed value 0.20 of the depolarization ratio ρ_v for benzene at 25 °C and λ_0 = 514.5 nm is 0.33 and appreciably smaller than our established value 0.41 ± 0.01 at λ_0 = 436 nm.[2,4] (Note that ρ_u and ρ_v of a given pure liquid are functions only of the pressure, temperature, and wavelength of the incident light as its absolute reduced intensities and never depend on the apparatus used and that those quantities are almost independent of the wavelength.) Thus the basis for their recommendation of the ellipsoidal Onsager–Scholte model seems to be weak. Considering the above circumstances, we have simply adopted the second-power-type correction as in the previous study.[1] This adoption is convenient for a comparison of the present results with the previous ones and also with literature data and may be considered to be sufficient for the present main purpose to analyze the dependence of $\langle\Gamma^2\rangle/x_w$ on x_w on the basis of the HW model.

The values of $\langle\Gamma^2\rangle/x_w$ for cumene and the three a-PS samples in CCl_4 at 25.0 °C calculated from eq 5 with the values $(\Delta R_{Hv,mol}/c)_{c=0}$ determined above are given in Table III along with those determined previously.[1] There are also given the values of the ratio of $\langle\Gamma^2\rangle$ for the a-PS samples to $\langle\Gamma^2\rangle_{(cumene)}$ for cumene. Although the present

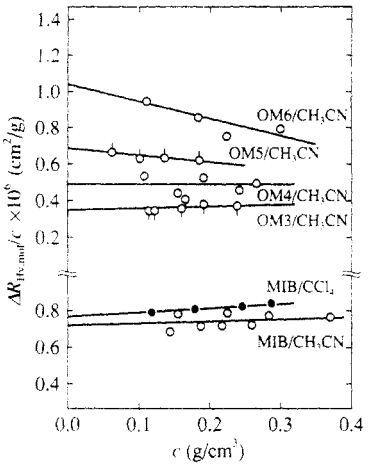

Figure 6. Plots of $\Delta R_{Hv,mol}/c$ against c for a-PMMA samples OM3 through OM6 and MIB in CH_3CN at 44.0 °C (○) and for MIB in CCl_4 at 25.0 °C (●).

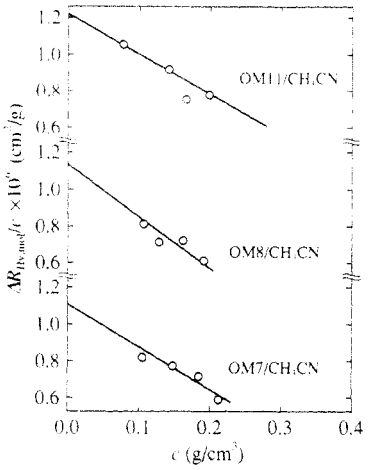

Figure 7. Plots of $\Delta R_{Hv,mol}/c$ against c for a-PMMA samples OM7 through OM11 in CH_3CN at 44.0 °C.

value of $\langle\Gamma^2\rangle/x_w$ for each sample is about twice as large as the previous one, the values of the ratio $\langle\Gamma^2\rangle/\langle\Gamma^2\rangle_{(cumene)}$ are in good agreement with each other. The disagreement between the absolute values in the present and previous studies may be regarded as arising from some defects in the procedure of Carlson and Flory[8] adopted previously.[1] Fortunately, however, as seen from the above comparison, it may give the correct dependence on x_w of the ratio of $\langle\Gamma^2\rangle/x_w$ to its value $(\langle\Gamma^2\rangle/x_w)_\infty$ in the limit of $x_w \to \infty$. Thus the previous analysis of $\langle\Gamma^2\rangle/x_w$ on the basis of the HW chain is still valid, since its absolute values do not affect the determination of the basic HW model parameters. In the previous analysis for a-PS, the local polarizability tensor assigned to the contour of the HW chain was evaluated from the literature values of the bond polarizabilities and group polarizability tensors determined by Flory and his co-workers with the use of the procedure of Carlson and Flory. Thus, in order to correct the previous experimental and theoretical values of $\langle\Gamma^2\rangle$, it is sufficient to multiply both of them by the ratio γ^2 of its present to previous experimental values for cumene in CCl_4, which is equal to 1.9_4.

(ii) a-PMMA. Having made a comparison of the present results with the previous ones for a-PS, we now proceed to present results for a-PMMA. Figure 6 shows plots of $\Delta R_{Hv,mol}/c$ against c for the latter samples OM3 through OM6 and MIB in CH_3CN at 44.0 °C (Θ) and also for MIB in CCl_4 at 25.0 °C. Figures 7 and 8 show similar plots for samples OM7 through OM11 and for OM18 through OM30, respectively, in CH_3CN at 44.0 °C. The

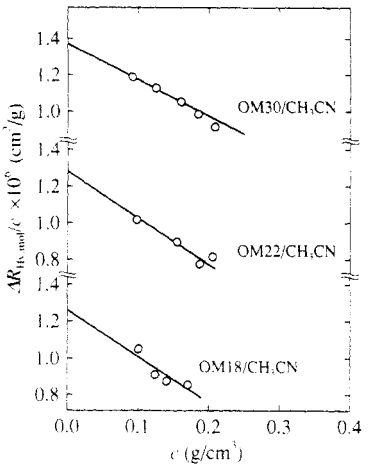

Figure 8. Plots of $\Delta R_{Hv,mol}/c$ against c for a-PMMA samples OM18 through OM30 in CH_3CN at 44.0 °C.

Table IV. Values of $\langle\Gamma^2\rangle/x_w$ for Atactic Oligo- and Poly(methyl methacrylate)s in Acetonitrile at 44.0 °C

sample	$\langle\Gamma^2\rangle/x_w$, Å^6	sample	$\langle\Gamma^2\rangle/x_w$, Å^6
MIB	4.1_6	OM8	6.4_7
OM3	1.9_9	OM11	6.9_5
OM4	2.8_0	OM18	7.1_7
OM5	3.9_2	OM22	7.2_9
OM6	5.9_3	OM30	7.8_0
OM7	6.3_2		

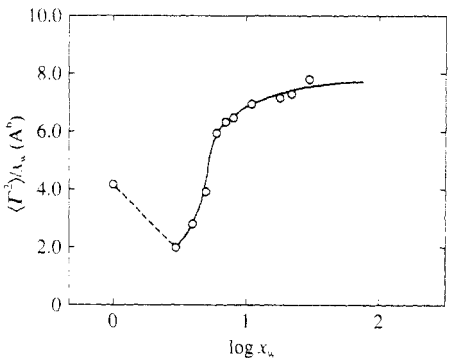

Figure 9. Plots of $\langle\Gamma^2\rangle/x_w$ against $\log x_w$ for the a-PMMA samples with $f_r = 0.79$ in CH_3CN at 44.0 °C (○). The solid curve connects smoothly the data points for $x_w \geq 3$.

data points for each sample follow a straight line as in the case of the a-PS samples in CCl_4 and can be extrapolated to infinite dilution to obtain $(\Delta R_{Hv,mol}/c)_{c=0}$. Except for the data for MIB in CCl_4, the relative errors in the extrapolation are somewhat larger than those for the a-PS samples.

The value of $\langle\Gamma^2\rangle$ for MIB in CCl_4 may be calculated from eq 5 with the value of $(\Delta R_{Hv,mol}/c)_{c=0}$ determined above and is obtained to be 3.7_2 Å^6, which is nearly twice as large as the value 2.0 Å^6 obtained by Flory et al.[24] with $\lambda_0 = 633$ nm at the volume fractions of the solute ranging from 0.3 to 1. This disagreement may be regarded as arising from the same source as in the case of cumene and a-PS.

The values of $\langle\Gamma^2\rangle/x_w$ determined for MIB and the a-PMMA samples in CH_3CN at 44.0 °C are listed in Table IV. The value 4.1_6 Å^6 of $\langle\Gamma^2\rangle$ for MIB, for which $\langle\Gamma^2\rangle = \langle\Gamma^2\rangle/x_w$, agrees fairly well with that in CCl_4, indicating that the effect of the optical anisotropy of CH_3CN is rather small if any, and $\langle\Gamma^2\rangle$ in CH_3CN has been determined successfully.

Dependence of $\langle\Gamma^2\rangle/x_w$ on x_w. Figure 9 shows plots of $\langle\Gamma^2\rangle/x_w$ against the logarithm of x_w for a-PMMA in CH_3CN at 44.0 °C (Θ). The solid curve connects smoothly the

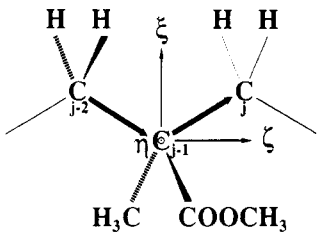

Figure 10. Localized Cartesian coordinate system assigned to the PMMA chain.

data points for $x_w \geq 3$, and the dashed line segment connects those for $x_w = 1$ and 3. It is seen that, as x_w is increased from unity, $\langle\Gamma^2\rangle/x_w$ (the mean-square optical anisotropy per repeat unit) is first reduced by half at $x_w = 3$, then increases very steeply up to $x_w \simeq 7$, and finally approaches a constant asymptotic value. From Figure 9, this value is estimated to be ca. 7.8 Å^6. The precise value is determined later through a comparison with the HW theory, but we only note here that it is about 1 order of magnitude smaller than the corrected corresponding value (ca. 61 Å^6)[1] for a-PS.

Discussion

Local Polarizability Tensor. Before proceeding to make a comparison of the present experimental results with the corresponding theory[13] on the basis of the HW chain, we must first assign a proper local polarizability tensor α per unit contour length to the chain. For this purpose, it is necessary to assign a localized Cartesian coordinate system (ξ, η, ζ) affixed to the HW chain to the repeat unit [CH_2–$C^\alpha(CH_3)(COOCH_3)$–CH_2] of the PMMA chain. The procedure of this assignment has already been established for both the isotactic (i-) and syndiotactic (s-) PMMA chains in the previous analysis[25] of the rotational isomeric state model[26] data for the angular correlation functions, as depicted in Figure 10. That is, for both i- and s-PMMA chains and therefore also for the a-PMMA chain, the ζ axis is taken along a line passing through the two successive methylene C atoms, the ξ axis is in the plane of the C–C^α and C^α–C bonds with its positive direction chosen at an acute angle with the $C^\alpha \rightarrow$C bond, and the η axis completes the right-handed system. We note that in the figure, the C–C^α bond is *l*-chiral and the C^α–C bond is *d*-chiral, following the new Flory convention[27] for describing stereochemical configurations of asymmetric chains.

Since the value of f_r of the present a-PMMA samples is rather close to unity, we adopt the polarizability tensor α_0 of the repeat unit of the s-PMMA chain for that of the former, for simplicity. If we assume the additivity of the bond and group polarizabilities, α_0 may be written as a sum of the contribution from the central part [C–$C^\alpha(CH_3)$-$(COOCH_3)$–C] and half of the contribution from the CH_2 groups on both sides. Strictly speaking, α_0 depends on the bond rotation angles around the bonds C–C^α and C^α–C, so that the α_0 averaged over the angles should be used. Because of the predominance of the *tt* conformation in the s-PMMA chain,[28] however, we may use the values of the components of α_0 for the *all-trans* conformation, for simplicity. By the use of the literature values of the bond polarizabilities[29-31] for C–C and C–H and of the polarizability tensor for methyl acetate or MIB,[24] which have been corrected by multiplying them by the common factor $\gamma = (1.9_4)^{1/2}$, the (traceless) α_0 for the repeat unit with the pair of successive bond chiralities *ld* as shown in Figure 10 may then be given by

$$\alpha_0 = \begin{pmatrix} 0.581 & -0.266 & 0 \\ -0.266 & 0.712 & 0 \\ 0 & 0 & -1.293 \end{pmatrix} \text{Å}^3 \qquad (6)$$

In the above evaluation of α_0, we have assumed that the plane of the ester group is perpendicular to the plane of the C–C^α and C^α–C bonds in the main chain and that the ester group occupies the possible two states in the former plane with equal probability. For the repeat unit with the pair of successive bond chiralities *dl*, α_0 is given by eq 6, with both the $\xi\eta$ and $\eta\xi$ components being 0.266 in place of −0.266.

In the s-PMMA chain, the pair of successive bond chiralities of the repeat unit and therefore the sign of the $\xi\eta$ and $\eta\xi$ components change alternately. Thus the values of α_0 obtained above cannot be adopted for α as it stands, since α to be assigned to the HW chain must be constant. In light scattering (with $\lambda_0 = 488$ nm), the fluctuation in the local polarizability tensor on the length scales of the repeat unit is immaterial, and it is sufficient to use the one averaged on somewhat longer length scales. We may then use α_0 with vanishing off-diagonal components, i.e.,

$$\alpha_0 = \text{diag}\,(0.581, 0.712, -1.293)\ \text{Å}^3 \qquad (7)$$

The tensor α may be calculated from

$$\alpha = (M_L/M_0)\alpha_0 \qquad (8)$$

with α_0 given by eq 7, where M_L is the shift factor as defined as the molecular weight per unit contour length and M_0 is the molecular weight per repeat unit.

Comparison with the HW Theory. Consider the HW chain of total contour length $L = M_0x/M_L$ (without excluded volume), whose conformational behavior may be described in terms of the three model parameters: the constant differential geometrical curvature κ_0 and torsion τ_0 of its characteristic helix taken at the minimum zero of its elastic energy and the static stiffness parameter λ^{-1}. Its $\langle\Gamma^2\rangle$ may be written in the form[1,13]

$$\langle\Gamma^2\rangle = \lambda^{-1}L\sum_{j=0}^{2} C_j(\alpha,\kappa_0/\nu,\tau_0/\nu)\, f_j(\lambda L,\lambda^{-1}\nu) \qquad (9)$$

where ν, C_j, and f_j are given by

$$\nu = (\kappa_0^{\,2} + \tau_0^{\,2})^{1/2} \qquad (10)$$

$$C_0(\alpha,x,y) = \frac{1}{2}[2\alpha_{\zeta\zeta} - \alpha_{\xi\xi} - \alpha_{\eta\eta} - 3x^2(\alpha_{\zeta\zeta} - \alpha_{\eta\eta}) + 6xy\alpha_{\eta\zeta}]^2$$

$$C_1(\alpha,x,y) = 6[xy(\alpha_{\eta\eta} - \alpha_{\zeta\zeta}) + (2y^2 - 1)\alpha_{\eta\zeta}]^2 + 6(x\alpha_{\xi\eta} + y\alpha_{\zeta\xi})^2$$

$$C_2(\alpha,x,y) = \frac{3}{2}(\alpha_{\xi\xi} - y^2\alpha_{\eta\eta} - x^2\alpha_{\zeta\zeta} + 2xy\alpha_{\eta\zeta})^2 + 6(y\alpha_{\xi\eta} + x\alpha_{\zeta\xi})^2 \qquad (11)$$

$$f_j(x,y) = (j^2y^2 + 36)^{-2}\{6(j^2y^2 + 36) + (j^2y^2 - 36)x^{-1} + x^{-1}e^{-6x}[(36 - j^2y^2)\cos(jxy) - 12jy\sin(jxy)]\} \qquad (12)$$

with α_{ij} ($i, j = \xi, \eta, \zeta$) being the ij component of the tensor α. It is convenient for the analysis of the experimental data to use the tensor α_0 instead of α. We then have from

eqs 8 and 9

$$\langle\Gamma^2\rangle/x = (\lambda^{-1}M_L/M_0)\sum_{j=0}^{2} C_j(\alpha_0,\kappa_0/\nu,\tau_0/\nu)\, f_j(\lambda L,\lambda^{-1}\nu) \quad (13)$$

where the reduced contour length λL is related to x_w by the equation

$$\log x_w = \log(\lambda L) + \log(\lambda^{-1}M_L/M_0) \quad (14)$$

Thus the quantity $\lambda^{-1}M_L$ may in general be estimated from a best fit of the theoretical curve of $\langle\Gamma^2\rangle/x$ against the logarithm of λL for properly chosen values of $\lambda^{-1}\kappa_0$ and $\lambda^{-1}\tau_0$ to the plot of the observed $\langle\Gamma^2\rangle/x_w$ against the logarithm of x_w.

Unfortunately, however, the shape of the theoretical curve calculated from eq 13 with α_0 given by eq 7 is rather insensitive to changes of $\lambda^{-1}\kappa_0$ and $\lambda^{-1}\tau_0$ around their respective values 4.0 and 1.1, which have been determined from an analysis of $\langle S^2\rangle$ in the previous study.[2] Then, as mentioned in the Introduction, it is difficult to determine unambiguously all the HW model parameters from an analysis of the present data for $\langle\Gamma^2\rangle$. Thus we only make a comparison of the data with the HW theoretical values calculated from eq 13 with the previous parameter values[2] from $\langle S^2\rangle$,[2] i.e., $\lambda^{-1}\kappa_0 = 4.0$, $\lambda^{-1}\tau_0 = 1.1$, $\lambda^{-1} = 57.9$ Å, and $M_L = 36.3$ Å^{-1}.

If we use α_0 given by eq 7, the HW theoretical value of the ratio $\langle\Gamma^2\rangle/x_w$ in the limit of $x_w \to \infty$, which we designate by $(\langle\Gamma^2\rangle/x_w)_\infty$, is calculated to be 14.3 Å^6. This is appreciably larger than its present experimental value of ca. 7.8 Å^6. This discrepancy clearly indicates that the values of α_0 used above are not appropriate. Since the value of $\langle\Gamma^2\rangle/x_w$ for the sample OM3 (trimer) is appreciably smaller than that for MIB (monomer) as shown in Figure 9, the values of the group polarizability tensor for the ester group estimated from the polarizability tensor of methyl acetate or MIB may be considered to be somewhat altered in the a-PMMA chain. Thus we multiply the above α_0 by a factor to obtain good agreement between theory and experiment, keeping the relative values of its diagonal components unchanged. Note that this modification preserves the orientation of its principal axes with respect to the localized coordinate system and that it does not change the HW theoretical values of $(\langle\Gamma^2\rangle/x_w)/(\langle\Gamma^2\rangle/x_w)_\infty$. It is then found that a best fit of the plot of the theoretical $\langle\Gamma^2\rangle/x_w$ against $\log x_w$ to the experimental one is obtained if we replace α_0 by $0.73\alpha_0$ with the value 7.68 Å^6 for $(\langle\Gamma^2\rangle/x_w)_\infty$.

Figure 11 shows plots of $(\langle\Gamma^2\rangle/x_w)/(\langle\Gamma^2\rangle/x_w)_\infty$ against the logarithm of x_w with $(\langle\Gamma^2\rangle/x_w)_\infty = 7.68$ Å^6. The solid curve represents the HW theoretical values thus calculated. It is seen that the theory may explain qualitatively the steep increase in the experimental value in the range of x_w from 3 to 7 and that there is quantitative agreement between theory and experiment for $x_w \gtrsim 6$. This indicates that the HW theory may give a consistent explanation of the behavior of $\langle\Gamma^2\rangle$, $\langle S^2\rangle$, and also $[\eta]$ as functions of M_w.

Comparison with the a-PS Chain. For comparison, the previous results for the a-PS samples (filled circles) and cumene (filled triangle)[1] in cyclohexane at 34.5 °C are also shown in Figure 11 along with the best-fit HW theoretical values (dashed curve).[1] Here, we have used the (uncorrected) value 31.5 Å^6 for $(\langle\Gamma^2\rangle/x_w)_\infty$ for the a-PS chain. It is seen that there is a remarkable difference between a-PMMA and a-PS; the ratio $(\langle\Gamma^2\rangle/x_w)/(\langle\Gamma^2\rangle/x_w)_\infty$ decreases very steeply with decreasing x_w in the range of $\log x_w$ from ca. 0.5 to ca. 1 for the former. Clearly, this difference arises from that in the local chain conformation

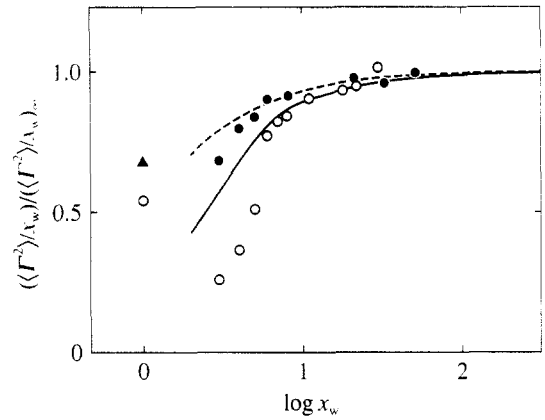

Figure 11. Plots of $(\langle\Gamma^2\rangle/x_w)/(\langle\Gamma^2\rangle/x_w)_\infty$ against $\log x_w$ for the a-PMMA samples with $f_r = 0.79$ (○) in CH_3CN at 44.0 °C and for the a-PS samples with $f_r = 0.59$ (●) and cumene (▲) in cyclohexane at 34.5 °C.[1] The solid and dashed curves represent the best-fit HW theoretical values for a-PMMA and a-PS, respectively.

between the two polymers, and the HW theoretical values may well reproduce this tendency. It is important to recall here that those for the a-PMMA chain have been calculated with the model parameters determined from $\langle S^2\rangle$, which can explain the observed maximum in $\langle S^2\rangle/M_w$.[2]

Concluding Remarks

The values of $\langle\Gamma^2\rangle$ determined for cumene and the three a-PS samples in CCl_4 at 25.0 °C by the use of the photometer equipped with the FP interferometer as a spectrometer have been found to be about twice as large as those determined previously.[1] This disagreement may be regarded as arising from some defects in the procedure of Carlson and Flory[8] adopted there. Fortunately, however, the only change to do in the previous analysis of the data on the basis of the HW chain is to multiply both the experimental and theoretical values of $\langle\Gamma^2\rangle$ by a common factor. Thus we do not have to revise the previous values of the ratio $(\langle\Gamma^2\rangle/x_w)/(\langle\Gamma^2\rangle/x_w)_\infty$ and therefore also of the HW model parameter for a-PS.[1]

The results for the a-PMMA samples in CH_3CN at 44.0 °C cannot be explained by the HW theory with the values of the model parameters determined previously from an analysis of $\langle S^2\rangle$, if we assume the local polarizability tensor α_0 for the repeat unit of the a-PMMA chain determined using the polarizability tensor of the ester group evaluated from that of methyl acetate or MIB[24] and properly corrected as above. This implies that the effective polarizability tensor of the ester group in the a-PMMA chain may be somewhat different from that in methyl acetate or MIB. Thus we have multiplied α_0 by an adjustable factor C to make the theoretical value of $(\langle\Gamma^2\rangle/x_w)_\infty$ coincide with the experimental one and found C to be 0.73. Then the theory may well explain the dependence of $\langle\Gamma^2\rangle/x_w$ on x_w for $x_w \gtrsim 6$, indicating that the model may give a consistent explanation of the behavior of $\langle\Gamma^2\rangle$, $\langle S^2\rangle$, and also $[\eta]$ as functions of M_w.

In general, there is some doubt whether we can determine accurately $\langle\Gamma^2\rangle$ of solute molecules in an optically anisotropic solvent. However, the present agreement between the two values of $\langle\Gamma^2\rangle$ for MIB in CH_3CN and in the optically isotropic solvent CCl_4 leads to the conclusion that the effect of the anisotropy of the solvent on the evaluation of $\langle\Gamma^2\rangle$ is rather small if any, as far as the solutions of a-PMMA in CH_3CN are concerned. Thus the dependence of $\langle\Gamma^2\rangle/x_w$ on x_w may give useful information about the local chain conformation also for a-PMMA.

Acknowledgment. This research was supported in part by a Grant-in-Aid (0143 0018) from the Ministry of Education, Science, and Culture, Japan. We thank Dr. T. Konishi for his assistance in the determination of R_{Hv} for pure benzene.

References and Notes

(1) Konishi, T.; Yoshizaki, T.; Shimada, J.; Yamakawa, H. *Macromolecules* **1989**, *22*, 1921 and succeeding papers.
(2) Tamai, Y.; Konishi, T.; Einaga, Y.; Fujii, M.; Yamakawa, H. *Macromolecules* **1990**, *23*, 4067.
(3) Fujii, Y.; Tamai, Y.; Konishi, T.; Yamakawa, H. *Macromolecules* **1991**, *24*, 1608.
(4) Abe, F.; Einaga, Y.; Yamakawa, H. *Macromolecules* **1991**, *24*, 4423.
(5) Yamada, T.; Yoshizaki, T.; Yamakawa, H. *Macromolecules* **1992**, *25*, 1487 and succeeding paper.
(6) Yamakawa, H. *Annu. Rev. Phys. Chem.* **1984**, *35*, 23.
(7) Yamakawa, H. In *Molecular Conformation and Dynamics of Macromolecules in Condensed Systems*; Nagasawa, M., Ed.; Elsevier: Amsterdam, The Netherlands, 1988; p 21.
(8) Carlson, C. W.; Flory, P. J. *J. Chem. Soc., Faraday Trans. 2* **1977**, *73*, 1505.
(9) Berne, B. P.; Pecora, R. *Dynamic Light Scattering*; Wiley: New York, 1976.
(10) Patterson, G. D. In *Methods of Experimental Physics*, Fava, R. A., Ed.; Academic Press: New York, 1980; Vol. 16A, p 170 and also papers cited therein.
(11) Fytas, G.; Patkowski, A.; Meier, G.; Fischer, E. W. *Macromolecules* **1988**, *21*, 3250 and succeeding papers.
(12) Patterson, G. D.; Griffiths, J. E. *J. Chem. Phys.* **1975**, *63*, 2406.
(13) Yamakawa, H.; Fujii, M.; Shimada, J. *J. Chem. Phys.* **1979**, *71*, 1611.
(14) Madden, P. A. *Mol. Phys.* **1978**, *36*, 365.
(15) Stevens, J. R.; Patterson, G. D.; Carroll, P. J.; Alms, G. R. *J. Chem. Phys.* **1982**, *76*, 5203.
(16) Hermans, J. J.; Levinson, S. *J. Opt. Soc. Am.* **1951**, *41*, 460.
(17) Bender, T. M.; Lewis, R. J.; Pecora, R. *Macromolecules* **1986**, *19*, 244.
(18) Horita, K.; Abe, F.; Einaga, Y.; Yamakawa, H. *Macromolecules*, submitted.
(19) Konishi, T.; Yoshizaki, T.; Yamakawa, H. *Macromolecules* **1991**, *24*, 5614.
(20) Yamada, T.; Yoshizaki, T.; Yamakawa, H. *Macromolecules* **1992**, *25*, 377.
(21) Berry, G. C. *J. Chem. Phys.* **1966**, *44*, 4550.
(22) Brunham, A. K.; Alms, G. R.; Flygare, W. H. *J. Chem. Phys.* **1975**, *62*, 3289.
(23) Einaga, Y.; Abe, F.; Yamakawa, H. *J. Phys. Chem.* **1992**, *96*, 3948.
(24) Flory, P. J.; Saiz, E.; Erman, B.; Irvine, P. A.; Hummel, J. P. *J. Phys. Chem.* **1981**, *85*, 3215.
(25) Yamakawa, H.; Shimada, J. *J. Chem. Phys.* **1979**, *70*, 609.
(26) Flory, P. J. *Statistical Mechanics of Chain Molecules*; Interscience: New York, 1969.
(27) Flory, P. J.; Sundararajan, P. R.; DeBolt, L. C. *J. Am. Chem. Soc.* **1974**, *96*, 5015.
(28) Yoon, D. Y.; Flory, P. J. *Polymer* **1975**, *16*, 645.
(29) Suter, U. W.; Flory, P. J. *J. Chem. Soc., Faraday Trans. 2* **1977**, *73*, 1521.
(30) Patterson, G. D.; Flory, P. J. *J. Chem. Soc., Faraday Trans. 2* **1972**, *68*, 1098.
(31) Patterson, G. D.; Flory, P. J. *J. Chem. Soc., Faraday Trans. 2* **1972**, *68*, 1111.